The long non-coding RNA *MEG3* plays critical roles in the pathogenesis of cholesterol gallstone

Changlin Qian
Eastern Hepatobiliary Surgery Hospital
Hua Liu
Shanghai Jiao Tong University School of Medicine Affiliated Renji Hospital
Weijing Qiu
Shanghai Jiao Tong University School of Medicine Affiliated Renji Hospital
Jie Zhang
Shanghai Jiao Tong University School of Medicine Affiliated Renji Hospital
Zhiyong Shen
Shanghai Jiao Tong University School of Medicine Affiliated Renji Hospital
Yongjie Zhang (zhangyj_md@126.com)
Eastern Hepatobiliary Surgery Hospital

Research article

Keywords: cholesterol gallstone, animal modeling, library construction, differential expression analysis, enrichment analysis, competing endogenous RNA

Posted Date: March 5th, 2020

DOI: https://doi.org/10.21203/rs.3.rs-16206/v1

Abstract

Background: Cholesterol gallstone (CG) is the most common gallstone disease, which is induced by biliary cholesterol supersaturation. The purpose of this study is to investigate the pathogenesis of CG.

Methods: Sixteen mice were equally and randomly divided into model group and normal control group. The model group was fed with lithogenic diets to induce CG, and then gallbladder bile lipid analysis was performed. After RNA-seq library was constructed, differentially expressed mRNAs (DE-mRNAs) and differentially expressed lncRNAs (DE-lncRNAs) between model group and normal control group were analyzed by DESeq2 package. Using clusterProfiler package, enrichment analysis for the DE-mRNAs was carried out. Based on Cytoscape software, the protein-protein interaction (PPI) network and competing endogenous RNA (ceRNA) network were built.

Results: The mouse model of CG was successfully established, and then 181 DE-mRNAs and 33 DE-lncRNAs between model and normal groups were selected. For the down-regulated SCP2 , lipid hydroperoxide transport was enriched. Moreover, KDM4A was selected as a hub node in the PPI network, and MEG3 was taken as a key lncRNA in the regulatory network. Additionally, the miR-107-5p/miR-149-3p/miR-346-3p—MEG3 regulatory pairs and MEG3—PABPC4/CEP131/NUMB1 co-expression pairs existed in the regulatory network.

Conclusion: These RNAs might be related to the pathogenesis of CG.

Backgroud

Gallstone disease is a kind of biliary tract diseases, in which cholesterol gallstone (CG) is the most frequent type [1]. CG can be induced by dyslipidemia, overweigh, insulin resistance, obesity, and the changes in cholesterol homeostasis [2]. Genetic factors, lifestyle, and diet are considered to be correlated with the occurrence of CG, especially, high-sugar, high-fat, low-fiber, and low-vitamin diets can increase the risk of CG [3,4]. The formation of CG is based on the imbalances of cholesterol, bile acid, lecithin and other components in bile, which leads to biliary cholesterol supersaturation and crystallization [5]. CG is a common healthy problem worldwide, and its incidence has risen sharply over the past decades [6]. Therefore, the mechanisms CG should be further explored.

Some RNAs have been reported to be involved in the course of CG. For example, lower serum levels of retinol binding protein 4 (RBP4) are detected in CG and are related to gallstone formation, and RBP4 levels reduce independent of renal function in CG patients [7]. The lithogenic diet can result in significantly lower cholecystokinin A receptor (CCKAR) and caveolin-3 (CAV3) in the gallbladder and lower CAV3 in the liver, indicating that CAV3 and CCKAR may be implicated in CG [8]. Through mediating fatty acid and cholesterol metabolism, miR-122 plays important roles in the development and progression of gallstones [9,10]. Both miR-210 and its target ATPase phospholipid transporting 11A (ATP11A) are dysregulated in human gallstones, and ATP11A expression is negatively correlated with miR-210 expression in patients

with the disease [11]. However, more RNAs correlated with the pathogenesis of CG still need to be investigated.

Previous studies demonstrate that long non-coding RNA (lncRNA) exerts its biological effects in regulating gene expression by acting as a miRNA sponge [12,13]. In the present study, the mouse model of CG was established and gallbladder bile lipid analysis was carried out. After the RNA-seq library was constructed, the sequencing data were implemented with a series of bioinformatics analyses to explore the key RNAs and regulatory relationships in CG. Our findings might be helpful to further understand the molecular mechanisms of CG.

Methods

Animal modeling and sample collection

Totally, 16 C57 male mice were purchased from Beijing Vital River Laboratory Animal Technology Co., Ltd. (Beijing, China). The mice were fed with chow diets in specific pathogen free (SPF) laboratory animal room for one week. Then, the mice were randomly divided into model group (n = 8) and normal control group (n = 8). The model group was fed with lithogenic diets (containing 15% fat, 1% cholesterol, and 0.5% sodium cholate) (Jiangsu Xietong Pharmaceutical Bio-engineering Co., Ltd., Jiangsu, China) for 5 weeks. Meanwhile, the normal control group was fed with chow diets. After the mice were killed by the method of cervical dislocation, the liver, gallbladder and bile were isolated, photographed, and kept at -80 °C. The experiments were conducted in accordance with the guidelines of the university committee for animal welfare (Ren Ji Hospital, School of Medicine,Shanghai Jiao Tong University, Shanghai).

Gallbladder bile lipid analysis

According to the manufacturer’s instructions, the changes of total cholesterol (TCH), total bile acid (TBA), total bilirubin (TBL), and direct bilirubin (DBL) in bile were detected by corresponding kits (Nanjing Jiancheng Bioengineering Institute, Nanjing, China).

RNA-seq library construction and data preprocessing

Using Trizol reagent (Invitrogen, Shanghai, china), total RNA was extracted from four liver tissues from the model group and three liver tissues from the normal control group following the manufacturer's manual. Then, the integrity and purity of the total RNA were detected by Agarose Gel Electrophoresis and spectrophotometer (Merinton, Beijing, China), respectively. After the RNA-seq library was established using the NEBNext® Ultra™ RNA Library Prep Kit for Illumina® (New England Biolabs, Beverly, MA, USA), library purification, library detection, library quantitation, and cBOT automatic clusters successively were conducted. Furthermore, sequencing was performed using the TruSeq SBS kit v4-HS (Illumina, San Diego, CA, USA).

Quality assessment of the sequencing data was performed by FastQC software [14] (version 0.10.1, https://github.com/pnnl/fqc). Using Cutadapt software [15] (version 1.9.1,

https://pypi.org/project/cutadapt/), the adapter sequences, the bases with mass value less than 20 or containing N at the 5 'or 3' ends, and the reads with length less than 75 bp were filtered out. Subsequently, the clean data was compared with the reference genome using Hisat2 software [16] (version 2.0.1, http://www.psc.edu/user-resources/software/hisat2, default parameters).

Differential expression analysis and enrichment analysis

Using DESeq2 package [17] (http://www.bioconductor.org/packages/release/bioc/html/DESeq.html) in R, differential analysis between model group and normal control group was carried out. The mRNAs with the adjusted p-value < 0.05 and $|\log_2$ fold change (FC)| > 1 were selected as the differentially expressed mRNAs (DE-mRNAs). The lncRNAs with p-value < 0.05 and $|\log_2$ FC| > 1 were taken as the differentially expressed lncRNAs (DE-lncRNAs). Using pheatmap package [18] (https://cran.r-project.org/web/packages/pheatmap/) in R, hierarchical clustering analysis was performed and clustering heatmap was drew.

Based on clusterProfiler package [19] (http://bioconductor.org/packages/release/bioc/html/clusterProfiler.html) in R, Gene Ontology (GO) and Kyoto Encyclopedia of Genes and Genomes (KEGG) enrichment analyses for the DE-mRNAs were implemented. The threshold for selecting the significant results was the p-value < 0.05.

Protein-protein interaction (PPI) network analysis

Under the threshold of PPI score (medium confidence) > 0.4, PPI network analysis for the DE-mRNAs was conducted using STRING database [20] (http://string-db.org). Combined with Cytoscape software [21] (http://www.cytoscape.org/), the PPI network was constructed. The CytoNCA plug-in [22] (parameter: without weight; http://apps.cytoscape.org/apps/cytonca) in Cytoscape software was used to analysis the topology properties of network nodes. The hub nodes [23] were selected according to Degree Centrality (DC), Betweenness centrality (BC), and Closeness centrality (CC) of network nodes.

Co-expression analysis and prediction of the genes targeted by miRNAs

Pearson correlation coefficients [24] of the DE-lncRNAs and the DE-mRNAs were calculated. The r > 0.95 and p-value < 0.05 were utilized for screening the significant results. Using miRanda database [25] (http://www.microrna.org), the miRNAs targeting the DE-lncRNAs and the DE-mRNAs were predicted. Under the thresholds of score > 1200 and energy < -150, the significant miRNA-lncRNA pairs and miRNA-mRNA pairs were selected.

Competing endogenous RNA (ceRNA) network analysis and selection of key lncRNAs

Combined with the lncRNA-mRNA co-expression pairs, the miRNA-lncRNA regulatory pairs, and the miRNA-mRNA regulatory pairs, the mRNA-miRNA-lncRNA regulatory relationships were obtained. Using

Cytoscape software [21], the ceRNA regulatory network was visualized.

According to the degrees of the lncRNAs in ceRNA regulatory network, the top 8 up-regulated lncRNAs and the top 8 down-regulated lncRNAs separately were selected as the key lncRNAs. Combined the lncRNA-mRNA co-expression pairs, the mRNAs co-expressed with the key lncRNAs were considered as the potential target genes of the key lncRNAs. To obtain the underlying functions of the key lncRNAs, enrichment analysis for these potential target genes was conducted using clusterProfiler package [19].

Results

Animal modeling and gallbladder bile lipid analysis

In the normal control group, the bile in the gall bladder of the mice was transparent and yellow. After five weeks of lithogenic diets, the gall bladder of the mice in the model group was larger than that in the normal group, and the bile was cloudy and darker. The results of gallbladder bile lipid analysis showed that TCH, TBA, TBL, and DBL levels in the model groups were all higher than those in the normal control group (Figure 1). These suggested that the mouse model of CG was successfully established.

Identification of DE-lncRNAs and DE-mRNAs

There were 181 DE-mRNAs (including 104 up-regulated mRNAs and 77 down-regulated mRNAs) and 33 DE-lncRNAs (including 17 up-regulated lncRNAs and 16 down-regulated lncRNAs) between model and normal groups. The clustering heatmaps for the DE-lncRNAs and the DE-mRNAs are shown in Figure 2.

For the up-regulated mRNAs, 419 GO_biological process (BP) terms, 86 GO_cellular component (CC) terms, and 134 GO_molecular function (MF) terms, and eight pathways were enriched (Figure 3A). For the down-regulated mRNAs, 229 GO_BP terms (such as lipid hydroperoxide transport (involving sterol carrier protein 2, *SCP2*)), 44 GO_CC terms, and 54 GO_MF terms, and seven pathways were enriched (Figure 3B).

PPI network analysis

After the PPI pairs for the DE-mRNAs were predicted, PPI network (involving 101 nodes and 116 edges) was constructed (Figure 4). According to DC, BC, and CC, protein tyrosine phosphatase receptor type C (PTPRC), lysine demethylase 4A (KDM4A), and spectrin alpha, non-erythrocytic 1 (SPTAN1) all were among the top 15 network nodes and were taken as the hub nodes (Table 1).

Co-expression analysis and prediction of the genes targeted by miRNAs

A total of 173 lncRNA-mRNA co-expression pairs were obtained, involving 24 lncRNAs and 96 mRNAs. For each lncRNA implicated in the co-expression pairs, enrichment analysis was conducted for its co-expressed mRNAs. Finally, 457 GO_BP terms, 80 GO_CC terms, and 137 GO_MF terms, and 11 pathways were enriched (Figure 5). Based on miRanda database, 9320 miRNA-lncRNA pairs (involving 1754

miRNAs and 19 lncRNAs) and 86 miRNA-mRNA pairs (involving 49 miRNAs and 10 mRNAs) were predicted.

CeRNA network analysis and selection of key lncRNAs

Combined with the mRNA-miRNA-lncRNA regulatory relationships, the ceRNA regulatory network (involving 24 up-regulated mRNAs, 53 down-regulated mRNAs, 11 up-regulated lncRNAs, 11 down-regulated lncRNAs, and 47 miRNAs) was built (Figure 6). There were 42 miRNA-mRNA regulatory pairs, 127 miRNA-lncRNA regulatory pairs, and 115 lncRNA-mRNA co-expression pairs in the ceRNA regulatory network.

Based on the degrees of the lncRNAs in the regulatory network, the top eight up-regulated lncRNAs (RIKEN cDNA 4933407K13 gene, *4933407K13Rik*; RIKEN cDNA 4833418N02 gene, *4833418N02Rik*; predicted gene 8378, *Gm8378*; RIKEN cDNA F730311O21 gene, *F730311O21Rik*; RIKEN cDNA A530020G20 gene, *A530020G20Rik*; Opa interacting protein 5, opposite strand 1, *1700020I14Rik*; RAB10, member RAS oncogene family, opposite strand, *Rab10os*; and predicted gene, 16973, *Gm16973*) and the top eight down-regulated lncRNAs (predicted gene 15270, *Gm15270*; maternally expressed 3, *MEG3*; RIKEN cDNA C730036E19 gene, *C730036E19Rik*; predicted gene 16576, *Gm16576*; predicted gene 27216, *Gm27216*; predicted gene 12655, *Gm12655*; predicted gene 11695, *Gm11695*; and predicted gene 6135, *Gm6135*) were screened out as the key lncRNAs. In the regulatory network, the *miR-107-5p/miR-149-3p/miR-346-3p—MEG3* regulatory pairs and *MEG3—PABPC4/CEP131/NUMB1* co-expression pairs existed. To predict the potential functions of these key lncRNAs, enrichment analysis for their co-expressed mRNAs was performed. Moreover, the enrichment results for four up-regulated lncRNAs (*4833418N02Rik*, *Gm8378*, *1700020I14Rik*, and *Gm16973*) and three down-regulated lncRNAs (*Gm16576*, *Gm27216*, and *Gm12655*) are presented in Figure 7.

Discussion

After the mouse model of CG was successfully constructed, 181 DE-mRNAs (including 104 up-regulated mRNAs and 77 down-regulated mRNAs) and 33 DE-lncRNAs (including 17 up-regulated lncRNAs and 16 down-regulated lncRNAs) between model and normal groups were screened. Enrichment analysis showed that lipid hydroperoxide transport was enriched for the down-regulated SCP2. Through mediating SCP2 expression, ursodeoxycholic acid decreases bile lithogenicity and thereby prevents the formation of CG [26]. Thus, SCP2 might act in the pathogenesis of CG via participating in lipid hydroperoxide transport. In the PPI network, KDM4A was selected as a hub node according to DC, BC, and CC. KDM4 expression is reduced during the activation of hepatic stellate cells and its knockdown induces the low expression of miR-29, which may provide potential therapeutic approaches for liver fibrosis [27]. Through recruiting KDM4, SBP (S-ribonuclease binding protein) family protein (BRG1) activates β-catenin target genes and may contribute to hepatic homeostasis and liver repair [28]. These suggested that KDM4A might be correlated with the mechanisms of CG.

After the regulatory network was built, the top eight up-regulated lncRNAs and the top eight down-regulated lncRNAs (including MEG3) were screened out as the key lncRNAs based on their degrees. MEG3 suppresses cell proliferation and promotes cell apoptosis in gallbladder cancer, and up-regulating MEG3 may be applied for inhibiting the deterioration of the tumor [29]. MEG3 overexpression in mouse liver can destabilize Shp mRNA and induce cholestatic liver injury via interacting with polypyrimidine tract-binding protein 1 (PTBP1) [30]. Therefore, MEG3 might also play roles in the development of CG.

Moreover, the miR-107-5p/miR-149-3p/miR-346-3p—MEG3 regulatory pairs and MEG3—PABPC4/CEP131/NUMB1 co-expression pairs were found in the regulatory network. MiR-107 facilitates hepatic lipid accumulation, causes hyperglycemia and damages glucose tolerance, and thus miR-107 plays important roles in hepatic lipid accumulation [31,32]. MiR-149 is up-regulated in the HepG2 cells receiving the treatment of long-chain fatty acid (FFA) and contributes to lipogenesis in the HepG2 cells untreated with FFA, therefore, miR-149 serves as a promising target for treating non-alcoholic fatty liver disease [33,34]. MiR-346 expression in the peripheral blood mononuclear cells of primary biliary cirrhosis patients is down-regulated in relative to the healthy controls, which may be related to the pathogenesis of the disease [35]. Zinc finger protein 664 (ZNF664) and PABPC4 variants have different correlations with the high density liptein cholesterol (HDL-C) in adolescents and adults, which may be induced by developmental changes or environmental differences [36]. The rs4660293 in PABPC4 is related to serum TCH, HDL-C, low-density lipoprotein cholesterol (LDL-C) and apolipoprotein A-I (ApoAI) levels in the Mulao and Han populations, and a gender-specific correlation is found in these populations [37]. CEP131 overexpression promotes cell proliferation and migration in hepatocellular carcinoma through activating the phosphatidylinositol-3 kinase (PI3K)/AKT signaling pathway, therefore, CEP131 is an oncogene and a candidate prognostic marker in the disease [38]. Numb in bile in liver mediates cholesterol reabsorption, and the G595D substitution of Numb damages NPC1 like intracellular cholesterol transporter 1 (NPC1L1)-associated cholesterol reabsorption in humans with low blood LDL-C [39]. These indicated that the miR-107-5p/miR-149-3p/miR-346-3p—MEG3 and MEG3—PABPC4/CEP131/NUMB1 regulatory axises might be involved in the pathogenesis of CG.

Conclusion

In conclusion, 181 DE-mRNAs and 33 DE-lncRNAs between model and normal groups were identified. Besides, SCP2 and KDM4A might be implicated in the mechanisms of CG. Furthermore, the miR-107-5p/miR-149-3p/miR-346-3p—MEG3 and MEG3—PABPC4/CEP131/NUMB1 regulatory axises might play roles in the development and progression of CG. Nevertheless, these results still need to be validated by rigorous experiments.

Abbreviations

CG
Cholesterol gallstone

DE-mRNAs
differentially expressed mRNAs
DE-lncRNAs
differentially expressed lncRNAs
PPI
protein-protein interaction
ceRNA
competing endogenous RNA
lncRNA
long non-coding RNA
TCH
total cholesterol
TBA
total bile acid
TBL
total bilirubin
DBL
direct bilirubin

Declarations

Ethics approval and consent to participate

The study was approved by the university committee for animal welfare (Ren Ji Hospital, School of Medicine，Shanghai Jiao Tong University, Shanghai).

Consent for publication

Not applicable.

Availability of data and materials

Not applicable.

Competing interests

The authors declare that they have no conflict of interest.

Funding

Not applicable.

Authors' Contributions

CLQ designed the research and carried out the animal experiment, CLQ, HL, WJQ, JZ, ZYS performed the bioinformatics analysis, CLQ wrote the original manuscript, YJZ participated in the experimental design and revised the original manuscript. All authors have read and approved the final manuscript.

Correspondence to Yongjie Zhang

Acknowledgements

Not applicable.

References

1. Pasternak A, Bugajska J, Szura M, et al. Biliary polyunsaturated fatty acids and telocytes in gallstone disease. *Cell Transplantation.* 2017;26(1):125.
2. Chen Y, Kong J, Wu S. Cholesterol gallstone disease: focusing on the role of gallbladder. *Laboratory Investigation.* 2015;95(2):124-131.
3. Ciaula AD, Garruti G, Frühbeck G, et al. The Role Of Diet In The Pathogenesis Of Cholesterol Gallstones. *Curr Med Chem.* 2019;26(19):3620-3638.
4. Chang CM, Chiu THT, Chang CC, Lin MN, CL. L. Plant-Based Diet, Cholesterol, and Risk of Gallstone Disease: A Prospective Study. *Nutrients.* 2019;11(2):335.
5. Ciaula AD, Wang DQ-H, Portincasa P. An update on the pathogenesis of cholesterol gallstone disease. *Current Opinion in Gastroenterology.* 2018;34(2):71-80.
6. Portincasa P, Wang DQ. Effect of Inhibition of Intestinal Cholesterol Absorption on the Prevention of Cholesterol Gallstone Formation. *Med Chem.* 2017;13(5):421.
7. Wang SN, Yeh YT, Wang ST, et al. Decreased Retinol Binding Protein 4 Concentrations are Associated With Cholesterol Gallstone Disease. *J Formos Med Assoc.* 2010;109(6):422-429.
8. Xu GQ, Xu CF, Chen HT, Liu S, Yu CH. Association of caveolin-3 and cholecystokinin A receptor with cholesterol gallstone disease in mice. *World Journal of Gastroenterology.* 2014;20(28):9513-9518.
9. Li T, Francl JM, Boehme S, Chiang JYL. Regulation of cholesterol and bile acid homeostasis by the cholesterol 7α-hydroxylase/steroid response element-binding protein 2/microRNA-33a axis in mice. *Hepatology.* 2013;58(3):1111-1121.
10. Song KH, Li T, Owsley E, Chiang JYL. A putative role of micro RNA in regulation of cholesterol 7?-hydroxylase expression in human hepatocytes. *Journal of Lipid Research.* 2010;51(8):2223-2233.
11. Yang B, Liu B, Bi P, Wu T, Wang Q, Zhang J. An integrated analysis of differential miRNA and mRNA expressions in human gallstones. *Molecular BioSystems.* 2015;11(4):1004-1011.
12. Yuan Y, Ren X, Xie Z, Wang X. A quantitative understanding of microRNA-mediated competing endogenous RNA regulation. *Quantitative Biology.* 2016;4(1):47-57.
13. Zhang T, Huang W. Modelling Competing Endogenous RNA Networks. *Journal of Cancer Therapy.* 2015;06(7):622-630.

14. Brown J, Pirrung M, McCue LA. FQC Dashboard: integrates FastQC results into a web-based, interactive, and extensible FASTQ quality control tool. *Bioinformatics.* 2017;33(19):3137-3139.
15. Chen C, Khaleel SS, Huang H, Wu CH. Software for pre-processing Illumina next-generation sequencing short read sequences. *Source Code for Biology & Medicine.* 2014;9(1):8.
16. Keel BN, M. SW. Comparison of Burrows-Wheeler Transform-Based Mapping Algorithms Used in High-Throughput Whole-Genome Sequencing: Application to Illumina Data for Livestock Genomes1. *Frontiers in Genetics.* 2018;9:35.
17. Love MI, Huber W, Anders S. Moderated estimation of fold change and dispersion for RNA-seq data with DESeq2. *Genome Biology.* 2014;15(12):550.
18. Zhang X, Yao X, Qin C, Luo P, Zhang J. Investigation of the molecular mechanisms underlying metastasis in prostate cancer by gene expression profiling. *Experimental & Therapeutic Medicine.* 2016;12(2):925-932.
19. Yu G, Wang L-G, Han Y, He Q-Y. clusterProfiler: an R Package for Comparing Biological Themes Among Gene Clusters. *OMICS-A JOURNAL OF INTEGRATIVE BIOLOGY.* 2012;16(5):284-287.
20. Szklarczyk D, Morris JH, Cook H, et al. The STRING database in 2017: quality-controlled protein–protein association networks, made broadly accessible. *Nucleic Acids Research.* 2017;45(D1):D362-D368.
21. Kohl M, Wiese S, Warscheid B. Cytoscape: Software for Visualization and Analysis of Biological Networks. *Methods Mol Biol.* 2011;696:291-303.
22. Tang Y, Li M, Wang J, Pan Y, Wu F-X. CytoNCA: A cytoscape plugin for centrality analysis and evaluation of protein interaction networks. *Biosystems.* 2015;127:67-72.
23. Hsing M, Byler KG, Cherkasov A. The use of Gene Ontology terms for predicting highly-connected \"hub\" nodes in protein-protein interaction networks. *BMC Syst Biol.* 2008;2(1):80.
24. Schober P, Boer C, Schwarte LA. Correlation Coefficients: Appropriate Use and Interpretation. *Anesthesia & Analgesia.* 2018;126(5):1.
25. He JH, Han Z-P, Zou M-X, et al. Analyzing the LncRNA, miRNA, and mRNA Regulatory Network in Prostate Cancer with Bioinformatics Software. *Journal of Computational Biology A Journal of Computational Molecular Cell Biology.* 2018;25(2):146-157.
26. Cui N, Cui Y, Li Z, Zhang J, Zhao E. Ursodeoxycholic acid lowers bile lithogenicity by regulating SCP2 expression in rabbit cholesterol gallstone models. *Excli Journal.* 2012;11:593-603.
27. Kong M, Wu J, Fan Z, Chen B, Wu T, Xu Y. The histone demethylase Kdm4 suppresses activation of hepatic stellate cell by inducing MiR-29 transcription. *Biochemical and Biophysical Research Communications.* 2019;514(1):16-23.
28. Li N, Kong M, Zeng S, et al. Brahma related gene 1 (Brg1) contributes to liver regeneration by epigenetically activating the Wnt/β-catenin pathway in mice. *Faseb Journal Official Publication of the Federation of American Societies for Experimental Biology.* 2019;33(1):327-338.

29. Liu B, Shen ED, Liao MM, Hu YB, Chen WD. Expression and mechanisms of long non-coding RNA genes MEG3 and ANRIL in gallbladder cancer. *Tumor Biology.* 2016;37(7):9875-9886.
30. Zhang L, Yang Z, Trottier J, Barbier O, L. W. Long noncoding RNA MEG3 induces cholestatic liver injury by interaction with PTBP1 to facilitate shp mRNA decay. *Hepatology.* 2017;65(2):604-615.
31. Bhatia H, Pattnaik BK, Datta M. Inhibition of mitochondrial β-oxidation by miR-107 promotes hepatic lipid accumulation and impairs glucose tolerance in vivo. *International Journal of Obesity.* 2016;40(5):861-869.
32. Joven J, Espinel E, Rull A, et al. Plant-derived polyphenols regulate expression of miRNA paralogs miR-103/107 and miR-122 and prevent diet-induced fatty liver disease in hyperlipidemic mice. *Biochimica Et Biophysica Acta.* 2012;1820(7):894-899.
33. Xiao J, Lv D, Zhao Y, et al. miR-149 controls non-alcoholic fatty liver by targeting FGF-21. *Journal of Cellular & Molecular Medicine.* 2016;20(8):1603-1608.
34. An X, Yang Z, An Z. MiR-149 Compromises the Reactions of Liver Cells to Fatty Acid via its Polymorphism and Increases Non-Alcoholic Fatty Liver Disease (NAFLD) Risk by Targeting Methylene Tetrahydrofolate Reductase (MTHFR). *Medical Science Monitor International Medical Journal of Experimental & Clinical Research.* 2017;23:2299-2307.
35. Tan Y, Tengli P, Yun Y, et al. Serum MicroRNAs as Potential Biomarkers of Primary Biliary Cirrhosis. *Plos One.* 2014;9(10):e111424.
36. Middelberg RPS, Heath AC, Madden PAF, Montgomery GW, Martin NG, Whitfield JB. Evidence of Differential Allelic Effects between Adolescents and Adults for Plasma High-Density Lipoprotein. *Plos One.* 2012;7(4):e35605.
37. Wu J, Yin R-X, Guo T, et al. Gender-specific association between the cytoplasmic poly(A) binding protein 4 rs4660293 single nucleotide polymorphism and serum lipid levels. *Molecular Medicine Reports.* 2015;12(3):3476-3486.
38. Liu XH, Yang YF, Fang HY, Wang XH, Wu DC. CEP131 indicates poor prognosis and promotes cell proliferation and migration in hepatocellular carcinoma. *International Journal of Biochemistry & Cell Biology.* 2017;90:1-8.
39. Wei J, Fu ZY, Li PS, et al. The Clathrin Adaptor Proteins ARH, Dab2 and Numb Play Distinct Roles in NPC1L1- versus LDL Receptor-mediated Cholesterol Uptake. *J Biol Chem.* 2014;289(48):33689-33700.

Table

Table 1. The top 15 Protein-protein interaction (PPI) network nodes according to Degree Centrality (DC), Betweenness centrality (BC), and Closeness centrality (CC).

Gene_id	DC	Gene_id	BC	Gene_id	CC
Cdc26	7	Ptprc	2964	Ptprc	0.032425
Ubr4	6	Ctss	2853	Ctss	0.032415
Kdm4a	5	Kdm4a	2569.333	Esr1	0.032196
Rps4x	5	Esr1	2448	Sptan1	0.032175
Fbxl8	5	Sptan1	2151	Mov10	0.031939
Spsb2	5	Triobp	1740	Kdm4a	0.031928
Ptprc	5	Cdc42bpa	1652	Il7r	0.031857
Klhl3	5	Ppp1r12c	1560	Triobp	0.031746
Keap1	5	Mov10	1560	Lyn	0.031746
Epn1	5	Psmd4	1504	Chpt1	0.031686
Uty	4	Dhx9	1467.667	Epn1	0.031626
Wac	4	Alkbh1	1384	Add3	0.031596
Psmd4	4	Cdc26	1188	Arf4	0.031496
Adsl	4	Adsl	1182	Rassf1	0.031466
Sptan1	4	Uty	988	Dhx9	0.031456

Figures

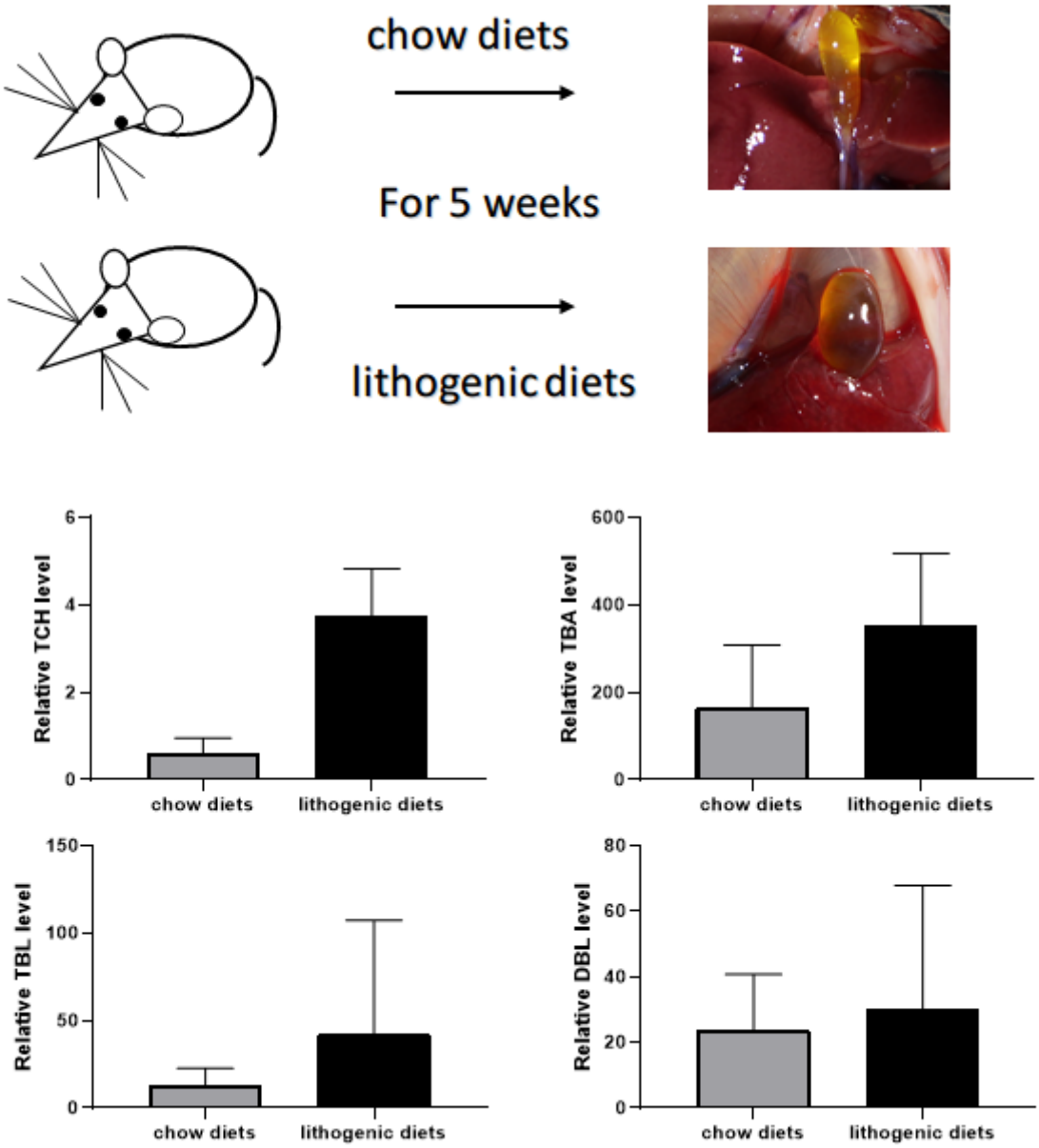

Figure 1

The results of animal modeling and gallbladder bile lipid analysis. TCH, total cholesterol; TBA, total bile acid; TBL, total bilirubin; DBL, direct bilirubin.

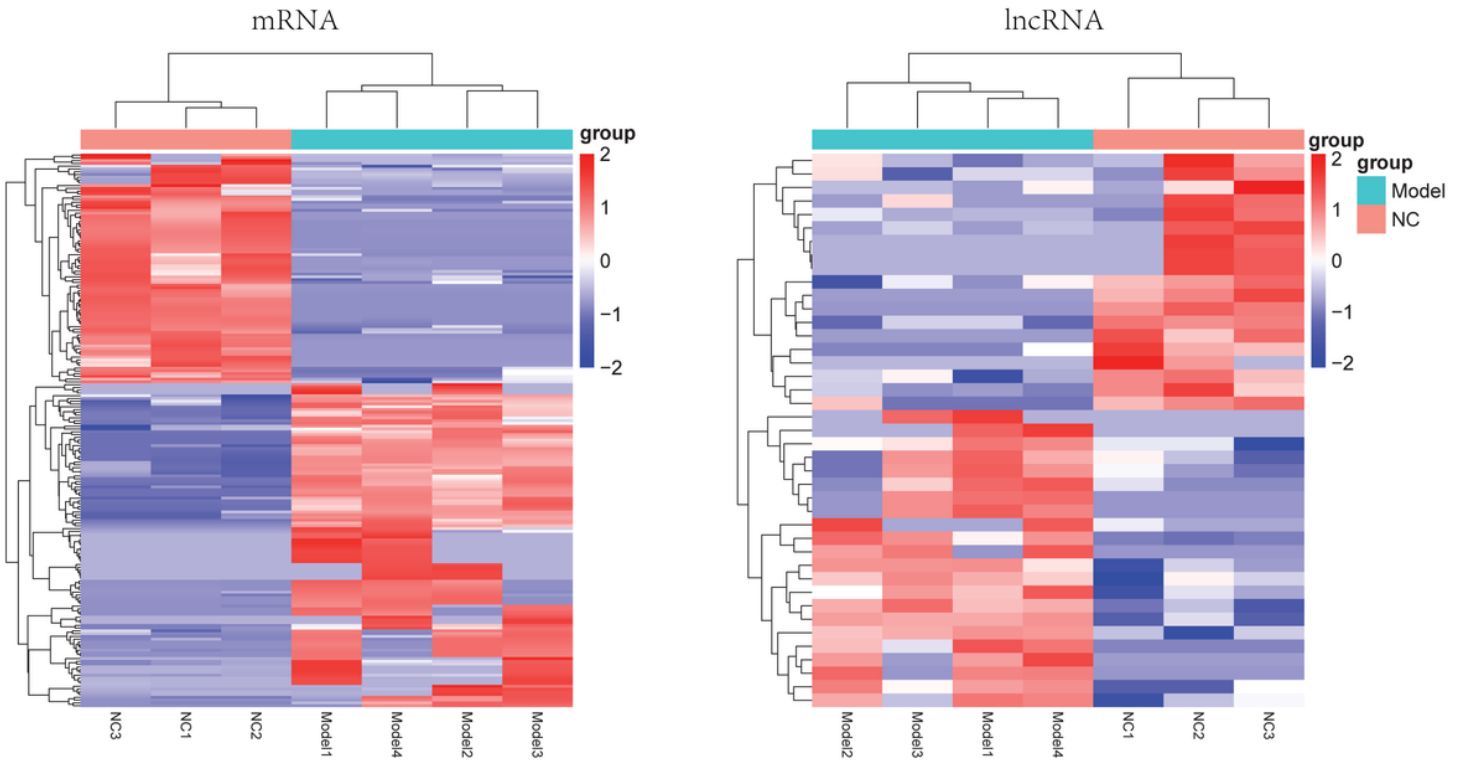

Figure 2

The clustering heatmaps for the differentially expressed mRNAs and the differentially expressed lncRNAs. In the sample strips, green and red separately represent model group and normal control (NC) group.

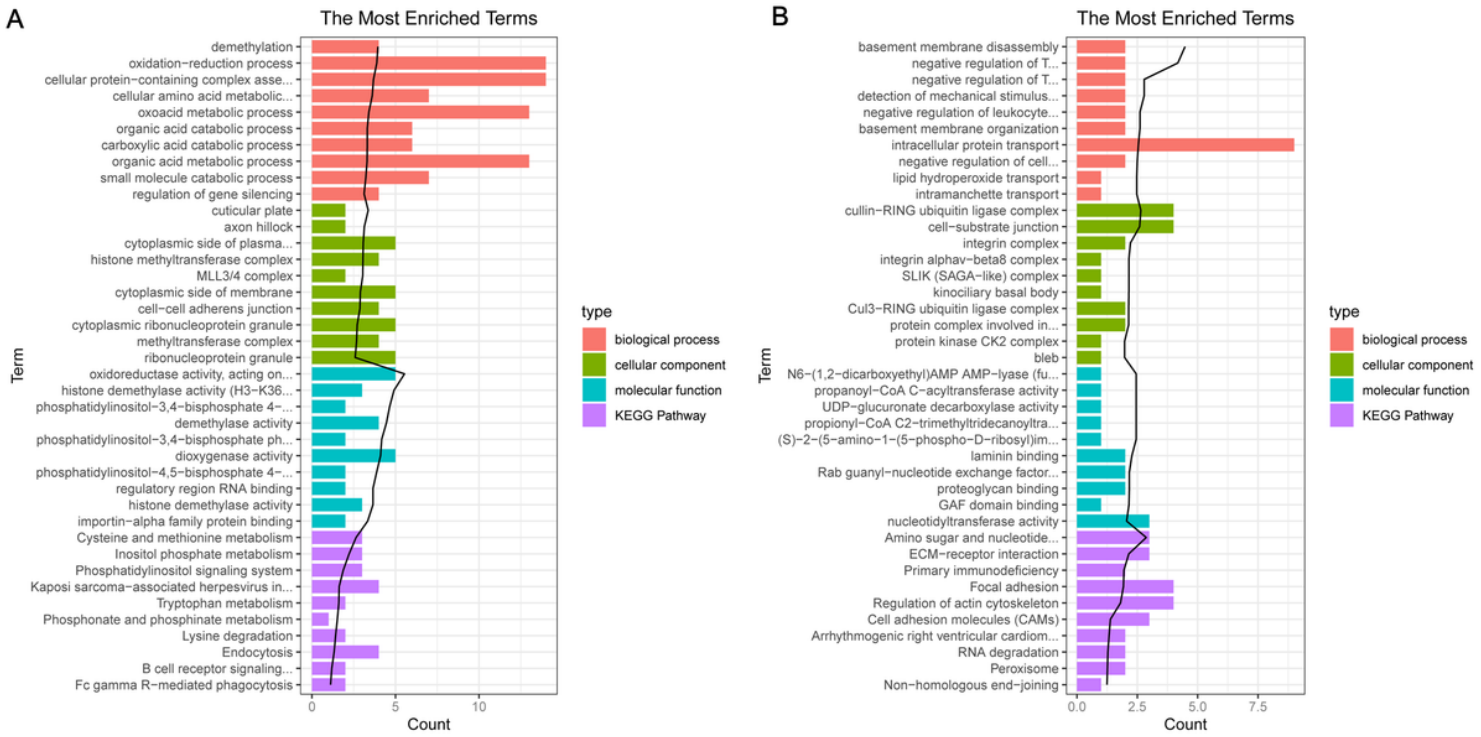

Figure 3

The enrichment results for the differentially expressed mRNAs (top 10 listed). (A) The enrichment results for the up-regulated mRNAs; (B) The enrichment results for the down-regulated mRNAs. Red, green, blue, and purple represent biological process terms, cellular component terms, molecular function terms, and Kyoto Encyclopedia of Genes and Genomes (KEGG) pathways, respectively.

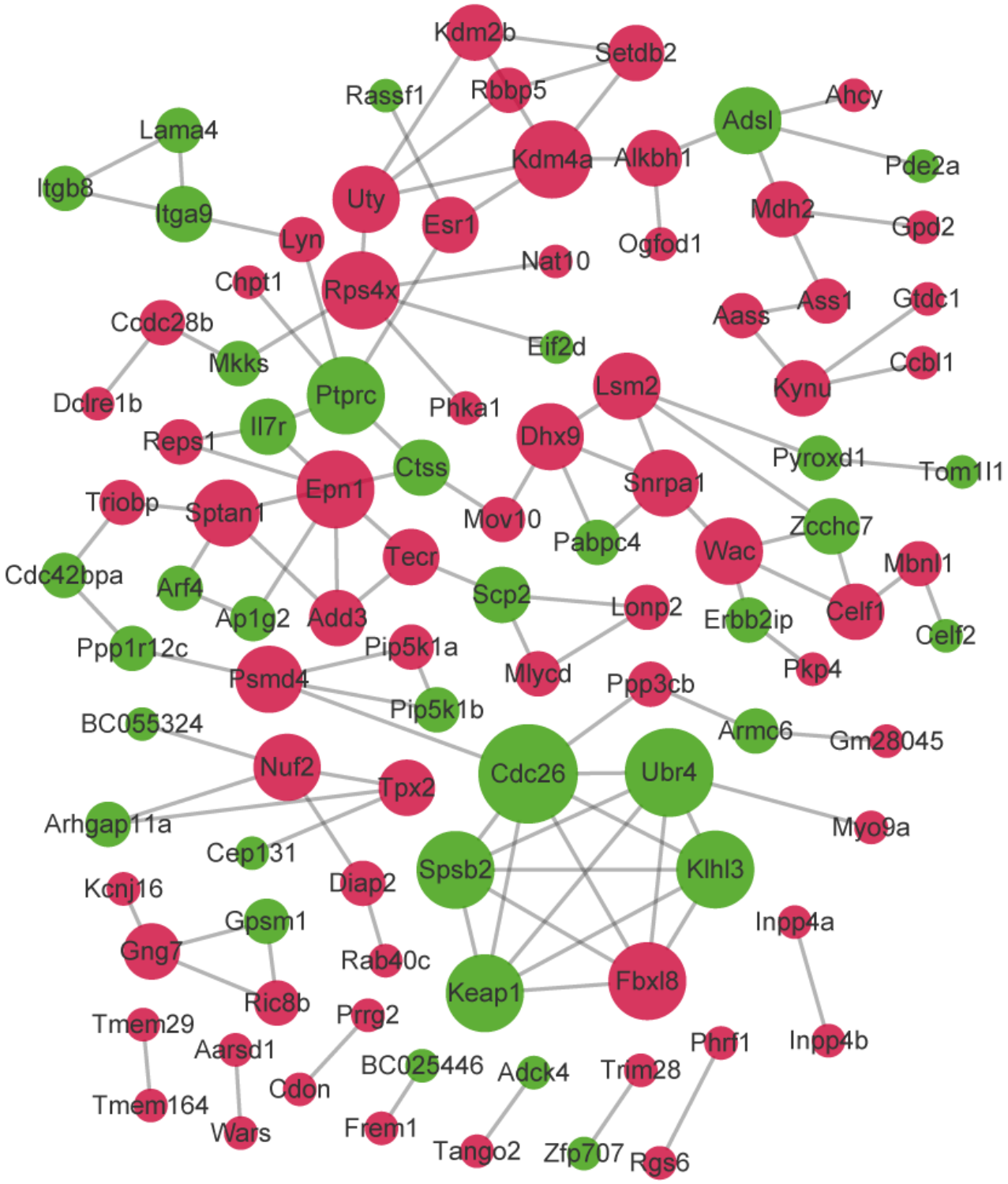

Figure 4

The protein-protein interaction network. Red and green circles separately represent up-regulated mRNAs and down-regulated mRNAs. The node size represents the connectivity degree.

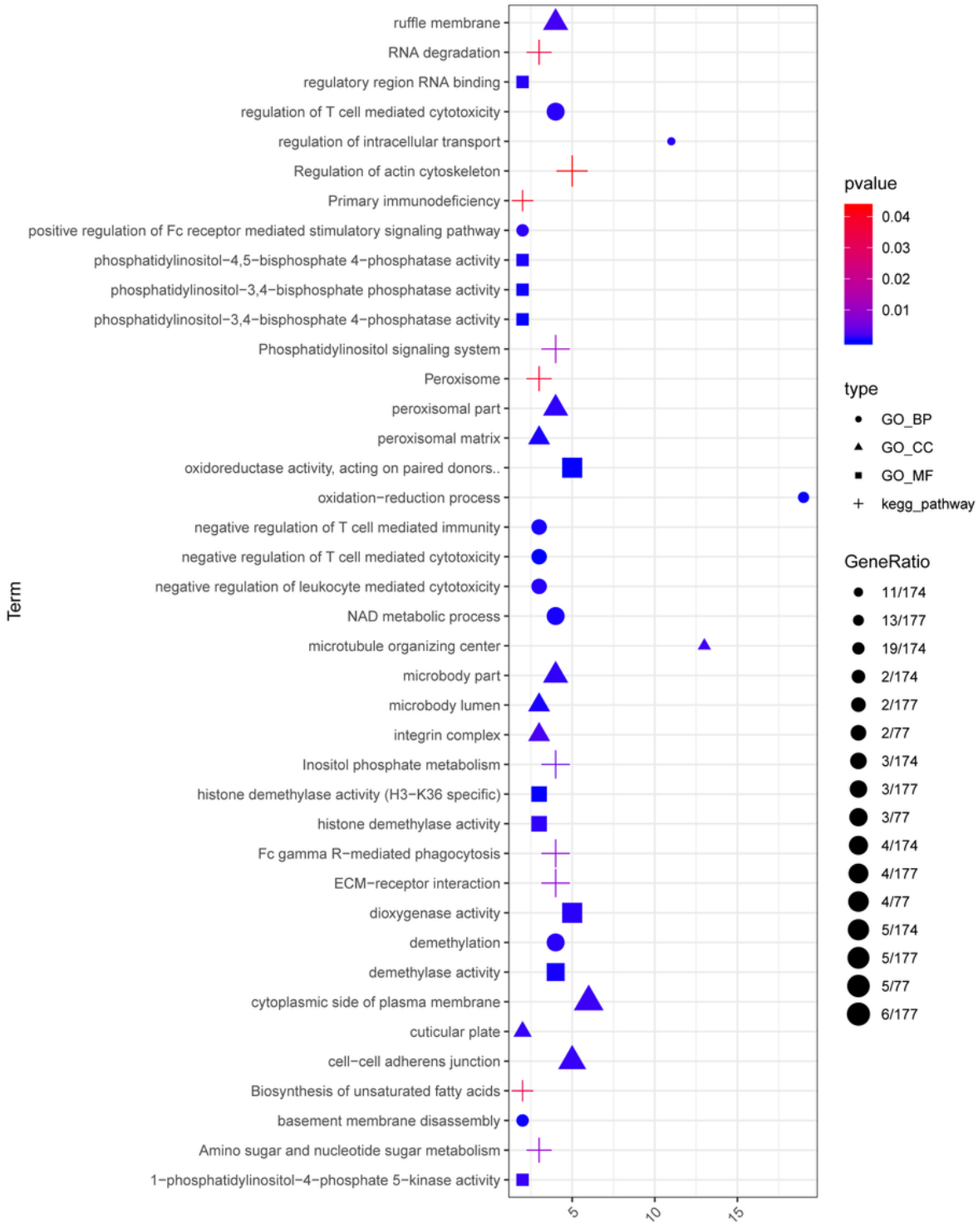

Figure 5

The enrichment results for the lncRNAs implicated in the co-expression pairs. Circles, triangles, squares, and crosses represent Gene Ontology (GO)_biological process (BP) terms, GO_cellular component (CC) terms, GO_molecular function (MF), and Kyoto Encyclopedia of Genes and Genomes (KEGG) pathways,

respectively. The color changing from red to blue indicates that the significant p-value decreases. The bubble size represents the proportion of the genes involved in one term.

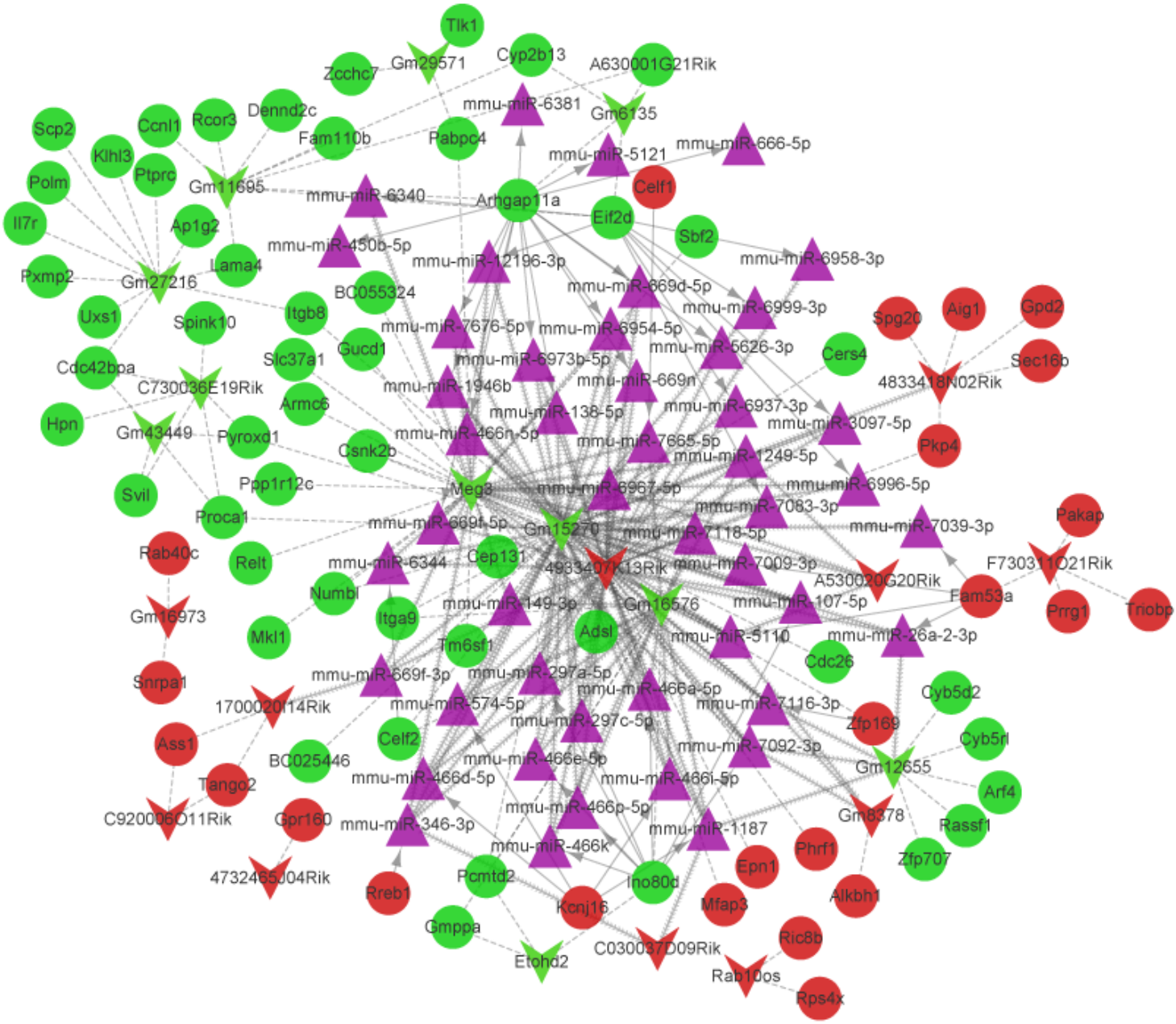

Figure 6

The competing endogenous RNA (ceRNA) network. Red and green separately represent up-regulation and down-regulation. Circles, inverted triangles, and purple regular triangles represent mRNAs, lncRNAs, and miRNAs, respectively. Dotted lines, fish scale lines, and the solid lines with arrows represent the lncRNA-mRNA co-expression pairs, the miRNA-lncRNA regulatory pairs, and the miRNA-mRNA regulatory pairs, respectively. The node size represents the connectivity degree.

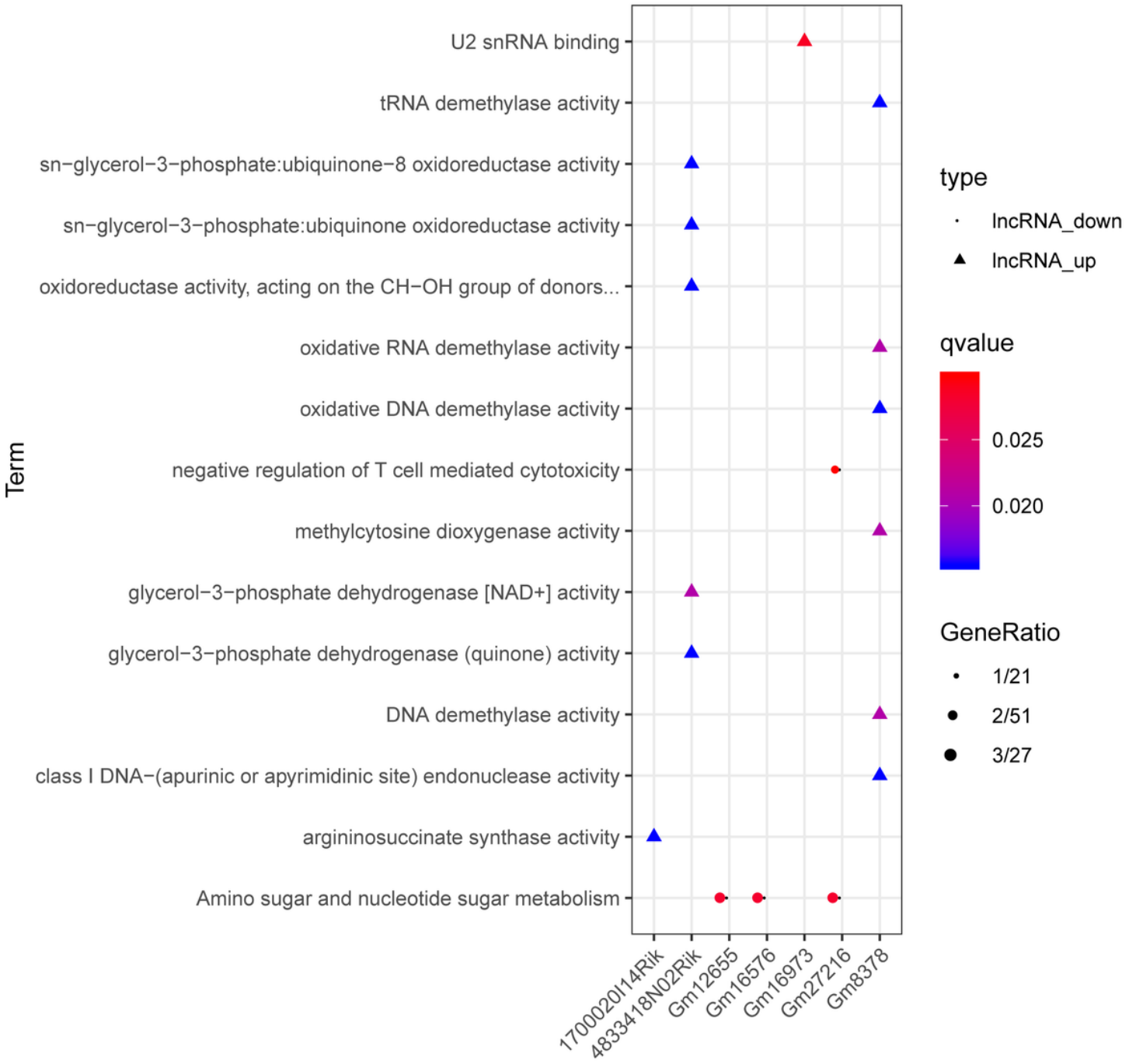

Figure 7

The enrichment results for up-regulated 4833418N02Rik, Gm8378, 1700020I14Rik, and Gm16973, and down-regulated Gm16576, Gm27216, and Gm12655. Triangles and circles represent up-regulated lncRNAs and down-regulated lncRNAs, respectively. The color changing from red to blue indicates that the significant p-value decreases. The bubble size represents the proportion of the genes involved in one term.